EXCLI Journal 2014;13:331-346 – ISSN 1611-2156
Received: January 31, 2014, accepted: February 27, 2014, published: April 01, 2014

Original article:

ENCAPSULATION OF CATECHIN AND EPICATECHIN ON BSA NPS IMPROVED THEIR STABILITY AND ANTIOXIDANT POTENTIAL

Ramdhan Yadav[1,2], Dharmesh Kumar[1], Avnesh Kumari[1], Sudesh Kumar Yadav[1,2,*]

[1] Biotechnology Division, CSIR-Institute of Himalayan Bioresource Technology, Palampur-176061 (H. P.), India
[2] Academy of Scientific and Innovative Research (AcSIR), New Delhi
* Corresponding author: sudeshkumar@ihbt.res.in; skyt@rediffmail.com

ABSTRACT

Nanoencapsulation of antioxidant molecules on protein nanoparticles (NPs) could be an advanced approach for providing stable, better food nutraceuticals and anticancer drugs. The bioavailability and stability of catechin (CAT) and epicatechin (ECAT) were very poor. In the present study, the CAT and ECAT were loaded on bovine serum albumin (BSA) NPs following desolvation method. The transmission electron microscope (TEM) and atomic force microscope (AFM) recorded size of CAT-BSA NPs and ECAT-BSA NPs were 45 ± 5 nm and 48 ± 5 nm respectively. The encapsulation efficiency of CAT and ECAT on BSA NPs was found to be 60.5 and 54.5 % respectively. CAT-BSA NPs and ECAT-BSA NPs show slow and sustained in vitro release. The CAT-BSA NPs and ECAT-BSA NPs were stable in solution at various temperatures 37 °C, 47 °C and 57 °C. DPPH assay revealed that CAT and ECAT maintained their functional activity even after encapsulation on BSA NPs. Furthermore, the efficacy of CAT-BSA NPs and ECAT-BSA NPs determined against A549 cell lines was found to be improved. CAT and ECAT aptly encapsulated in BSA NPs, showed satisfactory sustained release, maintained antioxidant potential and found improved efficacy. This has thus suggested their more effective use in food and nutraceuticals as well as in medical field.

Keywords: catechin, epicatechin, nanoparticles, bovine serum albumin, temperature stability, antioxidant activity

INTRODUCTION

Drug delivery through nanoparticles (NPs) is one of the most promising areas of nanotechnology. Nanoencapsulation is the formation of drug/molecule loaded NPs. Nanoencapsulation of drugs on NPs increases their efficacy, protects drug from degradation and maintains functional activity of encapsulated drugs (Reis et al., 2006). NPs used widely for drug delivery are fabricated from natural and synthetic macromolecules (Yadav et al., 2011; Kumari et al., 2010a). Among natural macromolecules, proteins have gained attention due to biodegradability, lack of toxicity and non-antigenicity (Moghimi et al., 2001; Patil, 2003; Maghsoudi et al., 2008). The presence of charged groups in proteins make them suitable matrix for drug entrapment (Zhao et al., 2010; Muller et al., 1996). Serum albumin from human and bovine have been commonly used for preparation of NPs. Albumin can accommodate large number of drugs in a non-specific manner and it can be prepared in large batches in simple and cost effective manner (Zhao et al., 2010). Many drugs like 5-fluorouracil, paclitaxel and sodium ferulate have been encapsulated on BSA NPs for improving

EXCLI Journal 2014;13:331-346 – ISSN 1611-2156
Received: January 31, 2014, accepted: February 27, 2014, published: April 01, 2014

their efficacy (Bansal et al., 2011; Li et al., 2008).

Bioactive agents such as nutrients, phytochemicals, nutraceuticals, cosmaceuticals may be incorporated into NPs to increase their efficacy and reduce their side effects (Yadav et al., 2013). The tea polyphenols catechin (CAT) and epicatechin (ECAT) having active hydroxyl groups are important for treating various diseases (Nagarajan et al., 2008) as well as for making anti-ageing beauty products (Maurya and Rizvi, 2009) and in food and nutraceutical applications. The molecular structures of CAT and ECAT are shown in Figure 1. Previous studies have reported that ECAT exert neuroprotective properties and prevent neuronal cell death, while the CAT is reported to be protective against induced cardio toxicity in rat (Inniguez-Franco et al., 2012). The widely consumed beverage tea has anti-tumorgenic, anti-oxidative, anti-mutagenic, anti-pathogenic properties due to the presence of CAT and ECAT (Maghsoudi et al., 2008; Chu et al., 2004). However, the over dose of CAT and ECAT for enhancing the bioavailability is not good for health and produces side effects and lowers the absorption of other bioactive molecules (Knekt et al., 1996). Likewise, the over consumption of hot tea containing CAT is responsible for acidity and prostate cancer (Koo and Cho, 2004; Shafique et al., 2012).

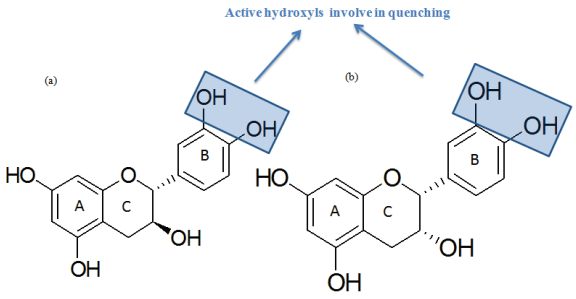

Figure 1: Molecular structures of (a) catechin (b) epicatechin

Inspite of wide spectrum biological properties of CAT and ECAT, their effective use is limited due to poor aqueous solubility, less stability and low bioavailability. The bioavailability of both these molecules is as low as 5 % (Catterall et al., 2003). Also the lack of long term stability (Volf et al., 2014), sensitivity to light and temperature (Munin and Edwards-Levy, 2011) are making these molecules unpopular in pharmaceutical and other industries. CAT encapsulated on PLGA NPs showed greater ability to scavenge free radicals (Pool et al., 2012). CAT encapsulated on gelatin NPs retained antioxidant activity even after three days of storage (Chen et al., 2010). NPs are commonly prepared by emulsification or desolvation method. But emulsification process requires the organic solvent removal and surfactant for emulsion stability, while desolvation method does not require organic solvent and surfactant. To overcome the problems of bioavailability, stability, self oxidation in water and side effects of overdose, CAT and ECAT loaded BSA NPs were synthesized in this study by desolvation method. Synthesized CAT-BSA, ECAT-BSA and blank-BSA NPs were characterised by nanodrop, TEM, DLS and FTIR. Encapsulation efficiency and drug loading was calculated with the help of HPLC. Temperature stability studies of CAT-BSA and ECAT-BSA NPs were also carried out at 37 °C, 47 °C and 57 °C. Antioxidant activity of synthesized CAT-BSA NPs and ECAT-BSA NPs was evaluated with DPPH assay. The efficacy analysis of pure CAT, ECAT and their loaded BSA NPs including blank NPs was carried out using the A549 cells.

MATERIAL AND METHODS

Materials

(+) Catechin and (-) epicatechin were purchased from Sigma (USA) and use as such. BSA was obtained from the New England Bio Lab (UK). The HPLC grade methanol and milli Q water were received from SD Fine Chemical Limited (India).

EXCLI Journal 2014;13:331-346 – ISSN 1611-2156
Received: January 31, 2014, accepted: February 27, 2014, published: April 01, 2014

Absolute ethanol (99.9 %) was purchased from Changshu Yanguan Chemical China.

The A549 (human lung carcinoma cells) cells were obtained from NCCS (National Centre for Cell Science), Pune and were cultured in HAM'S-F-12 (Sigma Aldrich), supplemented with 10 % heat inactivated fetal bovine serum (Sigma Aldrich) and 1 % antibiotic antimycotic (Sigma Aldrich). Cells were maintained at 37 °C in a 5 % CO_2 humidified atmosphere.

Preparation of CAT-BSA and ECAT-BSA loaded NPs

The synthesis of CAT and ECAT loaded and blank NPs of BSA was conducted using desolvation method. BSA (27 mg) was dissolved in 1 ml milli Q water in a 15 ml glass vials on magnetic stirrer at 37 °C. Absolute ethanol (3 ml) was added in 1 ml BSA along with CAT (4 mg) for generating the drug loaded NPs. Same method was followed for the synthesis of blank and ECAT loaded NPs. Gluteraldehyde (20 µl) was initially used for cross linking and synthesis of NPs. The synthesized NPs were left overnight after covering the vials with aluminum foils on magnetic stirrer at controlled conditions of 350 rpm and 37 °C. Next day, NPs were centrifuged at14000 rpm and redissolved in milli Q water for further use.

Characterization of synthesized BSA, CAT-BSA and ECAT-BSA NPs

Spectroscopic characterization

Two µl each of pure CAT, pure ECAT and CAT-BSA, ECAT-BSA and BSA NPs along with supernatant of CAT loaded BSA NPs and ECAT loaded BSA NPs (obtained after the removal of NPs by centrifugation) were used for spectroscopic analysis. The UV–Vis spectrophotometer (Nanodrop ND-2000 USA) with path length of 1 mm and 2048 element linear silicon CCD array detector was used for spectroscopic scan analysis from 220 to 700 nm using appropriate blanks.

Nicolet 6700 FTIR (Thermo, USA) spectrophotometer was used to record the IR spectra of pure CAT, pure ECAT and their loaded BSA NPs. The KBr pellets were prepared using the smart OMNI-sampler accessory at pressure of 125 Kg/ cm^2 for 3 min. Samples of IR were properly dried in oven for 5 days at 30 °C. The spectra of pure CAT, pure ECAT, CAT-BSA and ECAT-BSA NPs were analyzed in the scanning range of 400 -4000 cm^{-1} at 4 cm^{-1} resolution.

Surface morphological characterization

CAT, ECAT loaded BSA NPs and blank BSA NPs were characterized using the atomic force microscope (Nanoscope-III, Veeco Instruments, Singapore). A drop of NPs was put on the freshly clean glass surface, spread uniformly and left for drying in dust free conditions. Images were taken in tapping mode using silicon probe cantilever of 125 µm length, resonance frequency of 209-286 kHz, spring constant of 20-80 N/m and nominal, 5-10 nm tip radius of curvature and scan rate of 1 Hz. Each sample (BSA NPs, CAT-BSA NPs and ECAT-BSA NPs) was scanned with AFM silicon tips and minimum 3 images were recorded.

Finally, the synthesized NPs were characterized by the TEM (FEI, Netherlands) at a bias voltage of 200 kV. NPs dissolved in milli Q water were put on the carbon coated TEM grid and stained with two percent ammonium molybdate.

Thermo stability measurement of NPs

The stability of NPs in water was carried out at three temperatures 37 °C, 47 °C and 57 °C up to 72 h. The DLS size and zeta potential of blank-BSA NPs and loaded CAT-BSA and ECAT-BSA NPs were measured on DLS (Zetasizer Nano ZS, Malvern Instruments Ltd, UK) using disposable zeta cells. TEM images were recorded on carbon coated copper grid (CF300-Cu mesh, Electron Microscopy Sciences) using the negative stain ammonium molybdate.

EXCLI Journal 2014;13:331-346 – ISSN 1611-2156
Received: January 31, 2014, accepted: February 27, 2014, published: April 01, 2014

Encapsulation analysis of CAT- BSA and ECAT- BSA NPs with HPLC

HPLC (Waters USA, coupled with diode array detector 2998) was used to evaluate the encapsulation efficiency of CAT and ECAT molecules on BSA NPs. The supernatant (10 µl) of synthesized NPs obtained after centrifugation at 12000 rpm, was filtered through 0.22 µm membrane and directly injected in HPLC C18 column (150 mm × 4.6 mm, 5µm size) with the help of auto sampler (Waters 2707). Methanol and Milli-Q water (75 : 25) containing 0.1 % TFA were used as mobile phase with flow rate 0.8 ml/min at 280 nm. The calibration curves were generated using different concentrations of CAT and ECAT. The calibration curve of CAT was found linear in the range 0.0625 to 1 mg/ml and correlation coefficient was found as 0.999 ± 0.0002 (Figures S4(a) and (b)). Similarly the calibration curve of ECAT was linear in the range 0.0625 to 1 mg/ml and correlation coefficient was found 1 ± 0.0002 (Figures S4(c) and (d)). The regression equation generated by calibration curves of CAT ($Y = 1\times10^7x + 12915$) and ECAT ($Y= 1\times10^7x - 25467$) were used to calculate the encapsulation efficiency. The formulas given below were used for calculation of the encapsulation efficiency (EE) and the drug loading. (1)

$$EE(\%)=\left(\frac{amount\,of\,CAT/ECAT\,entrapped}{total\,amount\,of\,CAT/ECAT\,in\,formulation}\right)\times 100$$

(2)

$$CAT/ECAT\ loading(\%)=\left(\frac{mass\,of\,CAT/ECAT\,entrapped\,in\,nanoparticles}{mass\,of\,nanoparticles\,recovered\,after\,lyophilisation}\right)\times 100$$

In vitro release study of CAT- BSA and ECAT- BSA NPs

The release of CAT and ECAT from the NPs, during *in vitro* conditions was determined using HPLC. For the study of release kinetics, 10 mg CAT-BSA and ECAT-BSA NPs were dissolved in 20 ml of 0.1 M phosphate buffer saline (pH 7.4). The NPs solutions were continuously stirred at 50 rpm in thermostat to make the uniformity of NPs in buffer at constant temperature (37 °C). After regular intervals of 0, 2, 4, 6, 8, 12, 18, 24, 30, 36, 42 and 48 h, the samples were collected (1.0 ml) and lyophilized. The lyophilized samples were redissolved in methanol and centrifuged at 12000 rpm for 15 min. The samples were filtered through 0.22 µm membrane and injected in HPLC to analyze the release of CAT and ECAT in the buffer with help of calibration curves (Figures S4(a-d)).

The formula given below was used for the calculation of the amount of drug released at time‘t’ (3)

$$Cumulative\,release(\%)=\left(\frac{released\,amount\,of\,CAT/ECAT\,at\,time\,t}{total\,amount\,of\,CAT/ECAT\,at\,time\,t}\right)\times 100$$

Antioxidant activity analysis of encapsulated NPs

The 1,1-diphenyl-2-picrylhydrazyl free radical ($DPPH^{\bullet}$) was dissolved in methanol (3.9 mg/100 ml). The pure CAT, pure ECAT and NPs (ECAT-BSA, CAT-BSA and BSA NPs) were incubated with DPPH for half an hour in dark. The absorbance was recorded by the nanodrop (Nanodrop ND-2000 USA) at 517 nm in 2 ml optic glass cuvette and three replicates of each were used to evaluate the inhibition of DPPH. The blank BSA NPs were used as negative control and pure compounds (CAT/ECAT) were used as positive control. The formula given below was used to calculate the percentage of inhibition of DPPH by the test compounds pure CAT, pure ECAT, blank-BSA, CAT-BSA and ECAT-BSA NPs. (4)

$$Antioxidant\ activity\ (\%)=\left(\frac{(Absorbance\ of\ control)-(Absorbance\ of\ sample)}{(Absorbance\ of\ control)}\right)\times 100$$

Efficacy evaluation of BSA, CAT-BSA and ECAT-BSA NPs

The cellular efficacy of pure molecules vis-à-vis their encapsulated form was measured using the sulforhodamine B (SRB) method. Viable cells were seeded in the growth medium (100 µL) into 96 well microtiter plates (2×10^4 cells per well) and allowed to adhere overnight. The test compounds were dissolved in culture media and DMSO following 1:1 ratio respectively.

EXCLI Journal 2014;13:331-346 – ISSN 1611-2156
Received: January 31, 2014, accepted: February 27, 2014, published: April 01, 2014

Several dilutions starting from 50, 100, 150, and 200 µg/ml of CAT-BSA and ECAT-BSA NPs in 100 µl of complete medium were added to the selected wells. After dilution the plates were incubated at 37 °C for 24, 48 and 72 h using 5 % CO_2 incubator. After incubation period, 50 µL of 50 % trichloroacetic acid was added to the wells and then the plates were incubated at 4 °C for one hour. The TCA treated cells were washed 3 to 4 times with water and allowed to air dry. Subsequently, 100 µl of the SRB solution containing 1 % acetic acid was added to each well at room temperature. After standing for 30 min, the wells were washed 3 to 4 times with 1 % acetic acid and left for air dry. The bound dye was dissolved in 10 mM tris base (100 Ml / well). The absorbance was measured using microplate reader (BioTeK Synergy H1 Hybrid Reader) at wavelength of 540 nm. The percentage growth inhibition was calculated using the following formula: (5)

$$Cell\ \ inhibition\quad (\%) = 100 - \left(\frac{(At) - (Ab)}{(Ac - (Ab)} \right) \times 100$$

where Ab, Ac and At are absorbance value of blank, control and test compounds respectively.

RESULTS AND DISCUSSION

Loading of CAT and ECAT in BSA NPs

CAT and ECAT loaded BSA NPs were prepared by desolvation method. Desolvation is a thermodynamically driven self assembly process for proteins to form NPs. Size of NPs is controlled by varying protein content, pH, ionic strength, concentration of cross linking agent and amount of desolvating agent (Jun et al., 2011). This is a simple method for the synthesis of BSA NPs and there is no need of surfactants for capping the NPs surface. Also, size of BSA NPs can be controlled with this method (Zambaux et al., 1999). BSA was dissolved in milli Q (1 ml) water using magnetic stirrer. The ethanol containing CAT was added drop wise in BSA solution. This addition produced turbidity in reaction solution and resulted into the appearance of catechin-loaded BSA NPs in the solution. Ethanol acts as anti-solvent for BSA to reduce its solubility in water and facilitate NP formation by precipitation. NPs formed were crosslinked by glutaraldehyde. BSA has previously been used as synthesis materials for NPs and delivery of bioactive molecule (Xie et al., 2012). The synthesized NPs of CAT were separated and easily redispersed in the distilled water. Similarly ECAT loaded BSA NPs and blank BSA NPs were synthesized in solution form (Figure S1(k)). The dried CAT-BSA and ECAT- BSA and BSA NPs were stored at room temperature for further study.

Characterization of CAT-BSA and ECAT-BSA NPs

Spectroscopic characterization of CAT-BSA and ECAT-BSA NPs

UV–Vis spectrum is used for initial screening of synthesis of NPs (Yogasundaram et al., 2012). UV-Vis spectroscope ND 1000 was used to characterize the CAT and ECAT loaded BSA NPs. The UV-Vis characterization of BSA NPs gave a characteristic absorption peak at 230 nm and provided initial information about the synthesis of CAT-BSA NPs (Figure 2(a)) and ECAT-BSA NPs (Figure 2(b)).

FTIR spectroscopy was used to reveal the encapsulation of CAT and ECAT on BSA. The IR spectroscopy is not only used for the study of protein-protein interaction or with other molecules (Haris, 2010), but also used to analyze the encapsulation of bioactive molecules on the NPs. The IR spectroscopic analysis was used in the earlier study as well for the characterization of BSA NPs (Sailja and Amareshwar, 2012). The pure compounds CAT (Figure 3(a)) and ECAT (Figure 3(b)) and encapsulated CAT-BSA NP (Figure 3(c)) and ECAT-BSA NP (Figure 3(d)) were scanned using IR spectroscopy. The appearance of strong intensity bands at 3409.4, 3219.5 cm^{-1} represents -OH group, strong intensity bands at 1633.4, 1515.3 cm^{-1} represents aromatic C=

EXCLI Journal 2014;13:331-346 – ISSN 1611-2156
Received: January 31, 2014, accepted: February 27, 2014, published: April 01, 2014

C group, and medium intensity bands at 1143.5, 1019.7 cm^{-1} represents C-O-C group. The FTIR peaks of CAT loaded on BSA are in agreement with the IR spectra reported earlier for CAT, showing the characteristic absorption regions for -OH group (3400 – 3100 cm^{-1}), C = C group around 1600 cm^{-1}, as well as C-O-C group (1150 – 1010 cm^{-1}) (Maoela et al., 2009). The IR spectrum documented the loading of CAT in BSA NPs without any chemical interaction (Figure 3(c)). Similarly, the appearance of strong band at 3400.0 cm^{-1} represents -OH, strong intensity bands at 1653.9, 1523.4 cm^{-1} represents aromatic C = C, and medium intense bands at 1143.2 and 1094.7 cm^{-1} represents C-O-C (Figure 3(d)). The FTIR peaks of ECAT loaded on BSA are in agreement with the IR spectra reported earlier for ECAT, showing the characteristic absorption regions for -OH group (3362 cm^{-1}) and C = C groups (1600-1450 cm^{-1}) (Li et al., 2007). The IR spectrum documented the loading of ECAT in BSA NPs without any chemical interaction. FTIR has been used earlier in the study of conformational changes in albumin-gold nanoparticle bioconjugates (Shang et al., 2007). Also, the nanoencapsulation of bioactive molecules like quercetin and quercitrin on NPs have also been confirmed using FTIR (Kumari et al., 2010b, 2011).

Morphological characterization of CAT-BSA and ECAT-BSA NPs

NPs < 100 nm are of special interest for drug delivery. Size of NPs affects release rate, solubility and dissolution rate of a molecule/drug (Dufort et al., 2012). The targeting, stability, biocompatibility, and infiltration of the NPs inside the cellular tissues are also governed by the morphology and size of nanomaterials (Albanese et al., 2012). Smaller sized NPs are retained in systemic circulation for longer duration as compared to larger NPs (Nel et al., 2009). NPs undergo distribution to different organs of the body in size and shape dependent manner (Huang et al., 2010).

Size of CAT-BSA and ECAT-BSA NPs was measured by AFM and TEM. Blank BSA NPs were round, and spherical in nature (Figure 4(a)). AFM images revealed that surface morphology of the CAT-BSA NPs were round, smooth to polygonal (Figure 4(b)), while those of ECAT-BSA NPs were only round (Figure 4(c)). The CAT and ECAT loaded BSA NPs did not show aggregation (Figure 4(b) and 4(c)). Similar morphological characteristics have been reported earlier for CAT loaded PLGA and CAT loaded gelatin NPs (Pool et al., 2012;

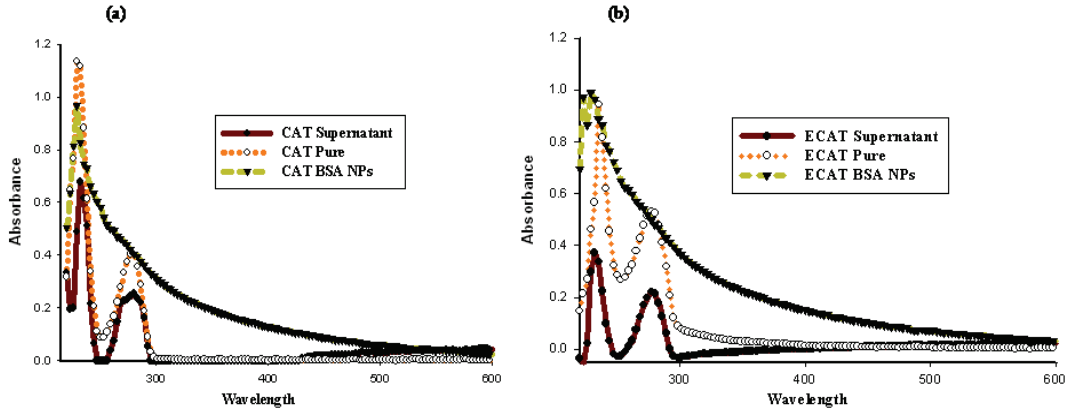

Figure 2: (a) UV–Vis spectra of pure catechin (CAT) and catechin-bovine serum albumin nanoparticles (CAT-BSA NPs) and catechin-bovine serum albumin (CAT-BSA) supernatant solution (left after the removal of synthesized CAT-BSA NPs), **(b)** UV–Vis spectra of pure epicatechin (ECAT), epicatechin-bovine surum albumin nanoparticles (ECAT-BSA NPs) and epicatechin-bovine serum albumin (ECAT-BSA) supernatant solution (left after the removal of synthesized ECAT-BSA NPs).

EXCLI Journal 2014;13:331-346 – ISSN 1611-2156
Received: January 31, 2014, accepted: February 27, 2014, published: April 01, 2014

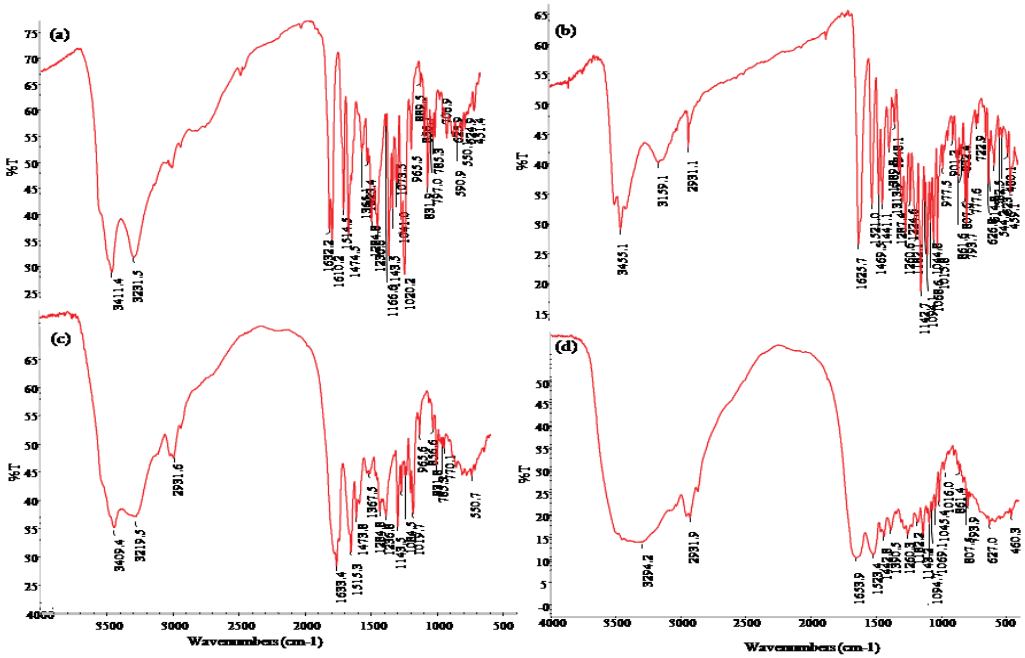

Figure 3: FTIR chromatogram of **(a)** pure catechin (CAT), **(b)** pure epicatechin (ECAT), **(c)** catechin-bovine serum albumin nanoparticles (CAT-BSA NPs), **(d)** epicatechin-bovine serum albumin nanoparticles ECAT-BSA NPs

Chen et al., 2010). TEM was used for further morphological characterization of NPs.

The CAT-BSA and ECAT-BSA NPs were smaller in size than blank-BSA NPs size (62 ± 10 nm) (Figure 4(d)). The average size of the CAT-BSA NPs and ECAT-BSA NPs were 45 ± 5 (Figure 4(e)) and 48 ± 5 nm (Figure 4(f)), respectively. The synthesized NPs were smooth, and spherical in shape. DLS was used to measure the zeta potential of CAT-BSA, ECAT-BSA and blank-BSA NPs. Zeta potential of CAT-BSA, ECAT-BSA and blank-BSA NPs were -34.6, -22.5 and -32.6 mV respectively.

Previous study has reported the formation of 410 nm size NPs of CAT with PLGA (Chen et al., 2010). However; in this study we could synthesize CAT-BSA and ECAT-BSA NPs of the size below 50 nm. Hence, these may find better potential for medical applications in comparison to the earlier reported CAT NPs on PLGA.

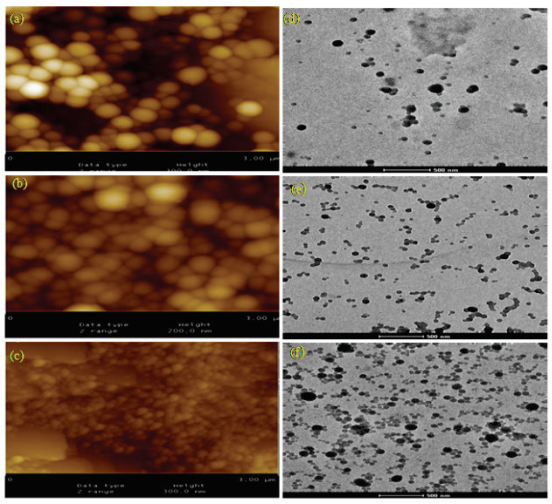

Figure 4: Shape and size analysis of blank-bovine serum albumin nanoparticles (BSA NPs), catechin-bovine serum albumin nanoparticles (CAT-BSA NPs) and epicatechin-bovine serum albumin nanoparticles (ECAT-BSA NPs). Atomic force microscope (AFM) images of **(a)** blank-BSA NPs, **(b)** CAT-BSA NPs, **(c)** ECAT-BSA NPs. Transmission electron microscope (TEM) images of **(d)** blank- BSA NPs, **(e)** CAT-BSA NPs, **(f)** ECAT-BSA NPs

EXCLI Journal 2014;13:331-346 – ISSN 1611-2156
Received: January 31, 2014, accepted: February 27, 2014, published: April 01, 2014

Nanoencapsulation provided thermostable and maintained antioxidant potential of CAT and ECAT in CAT-BSA and ECAT-BSA NPs

NPs stability is classified in terms of chemical stability, pharmaceutical stability, and physical stability. Although the pharmaceutical stability (Muthu and Feng, 2009) and chemical stability (Avgoustakis et al., 2002) have been assessed and different degradation mechanisms have been identified depending on NPs dimensions and polymer reactivity (von Burkersroda et al., 2002). The colloidal stability of NPs is still remained poorly investigated (Madlova et al., 2009). In the present study, physical stability of CAT-BSA, ECAT-BSA and BSA NPs was assessed in solution using the Zeta sizer and TEM at three temperatures 37 °C, 47 °C and 57 °C. The shape and surface morphology of NPs in solutions at different temperatures was monitored by TEM after 24, 48 and 72 h of incubation.

Earlier, BSA has been used as a stabilizer agent for the synthesis of stable nanoformulations of gold, silver and their alloy NPs (Singh et al., 2005). Zeta potential is a good indicator of physical stability of NPs (Kumari et al., 2012). Zeta potential values of CAT-BSA and blank-BSA NPs were decreased from -35.8 mV to -24.8 mV and -36.2 mV to -25.2 mV (Figure 5(a)) respectively after 72 hours of incubation at 37 °C. Temperature and light have also been reported earlier to decrease the zeta potential of solid lipid NPs (Freitas and Müller, 1998). However, the DLS size of the CAT-BSA and blank-BSA NPs was decreased from 187.2 nm to 176.2 nm and 250.6 to 229.7 nm (Figure 6(a)) respectively. The surface charge of ECAT-BSA NPs was increased from -46.3 mV to -48 mV (Figure 5(a)) within 48 h and then it become stable upto 72 h of incubation at 37 °C. A small reduction in size of ECAT-BSA NPs was observed after 72 h of incubation compared to blank-BSA NPs (Figure 6(a)). Still, the synthesized NPs were found to maintain their physical integrity and shape revealed by TEM recorded pictures (Figure S1).

Further the solution stability of NPs was checked at 47 °C. The size of blank as well as loaded NPs was reduced (Figure 6(b)) and surface charge was found to be remained stable (Figure 5(b)). The zeta potential of ECAT- BSA NPs was decreased to -36.8 from -46.2 mV at 47 °C (Figure 5(b)). The stability of NPs was also analyzed at higher temperature 57 °C for 3 days. The surface charge and size of NPs (blank and encapsulated NPs) were slightly changed in DLS analysis. However, the particles were observed to maintain their size and shape in TEM recorded pictures (Figure S3). The recorded size of NPs with TEM and DLS was different as reported in earlier study (Ma et al., 2012). DLS measures the hydrodynamic size of NPs. Hydrodynamic size tells about inorganic core along with coating material or the solvent layer attached to the NPs surface. While in dried NPs the hydration layer is not present and TEM measure the core of NPs. Hence, the hydrodynamic diameter is always greater than the actual size recorded by TEM (Ma et al., 2012).

The recorded pictures of CAT-BSA, ECAT-BSA and BSA NPs showed no sign of degradation and maintain their physical stability even after 72 h at 37 °C (Figure S1), 47 °C (Figure S2) and 57 °C (Figure S3). The surfactants sodium dodecyl sulfate (SDS), polyoxyethylenesorbitane monooleate (Tween 80) and polymer polyvinylpyrrolidone (PVP 360) have been reported to be altering the stability and surface of NPs (Kvıtek et al., 2008). Since CAT-BSA and ECAT-BSA NPs were synthesized without any of these surfactants use, they showed physical stability.

The CAT and ECAT get oxidized very quickly, leading to progressive appearance of a brown colour and unwanted odors with a considerable loss in antioxidant activity (Bark et al., 2011). Nanoencapsulation of CAT on chitosan tripolyphosphate NPs has been reported to maintain antioxidant activ-

EXCLI Journal 2014;13:331-346 – ISSN 1611-2156
Received: January 31, 2014, accepted: February 27, 2014, published: April 01, 2014

ity even after 24 h, while free CAT degraded in 8 h (Dube et al., 2010). To check the oxidation of nanoencapsulated CAT and ECAT on BSA NPs, the dissolved NPs were analyzed for their color. There was no change in the color of CAT-BSA NPs and ECAT-BSA NPs (Figure S1(k)); while the pure CAT and ECAT were found to be oxidized within a day and their color was changed from transparent to light yellowish (Figure S1(j)). The bound molecules with NPs were not oxidized whereas the unbound molecules in supernatant of CAT-BSA NPs and ECAT-BSA NPs were oxidized within 24 h (Figure S1(l)). Hence, nanoencapsulation might have provided protection to CAT and ECAT molecules from oxidation (Figure S1(k)). These results have proved that CAT and ECAT in the BSA NPs were stable at higher temperature for longer duration compared to pure CAT and ECAT. It might be protecting the bioactive molecules inside the tissue during temperature rise. This study further revealed that the molecules which are temperature sensitive can be delivered inside the body by encapsulating on the BSA NPs. It will minimize the chance of drug degradation as temperature rises in the body during hyperpyrexia (McGugan, 2001).

Analysis of CAT and ECAT loading in BSA NPs

The encapsulation efficiency depends on type of methods, type of molecule, encapsulating materials (synthetic and natural) and medium of NPs synthesis (Elzoghby et al., 2012). The encapsulation efficiency (EE) of CAT and ECAT on BSA NPs was carried out using the modified validated HPLC method (Li et al., 2012). The EE was calculated by formula 1. The EE of CAT was found 60.5 %, while that of ECAT-BSA NPs was 54 %. The unbound drug appeared in supernatant was detected by HPLC (Figure S5).

As chemical structures of the two molecules are different in stereochemistry, it could produce difference in EE on BSA NPs. The loading of CAT and ECAT on BSA NPs was calculated using formula 2 and found 12.73 % for CAT and 10.9 % for ECAT. On the other hand the EE of 9-nitrocamptothecin on PLGA NPs has been reported more than 30 % (Derakhshandeh et al., 2007). Gemcitabine has been loaded in BSA-PLGA (dl-lactide-co-glycolide) based core-shell NPs with an EE of 40.4 % (Chitkara and Kumar, 2013). The reported EE of doxorubicin was 88.24 % in cationic albumin NPs and was achieved by desolvation method (Abbasi et al., 2012). Hence,

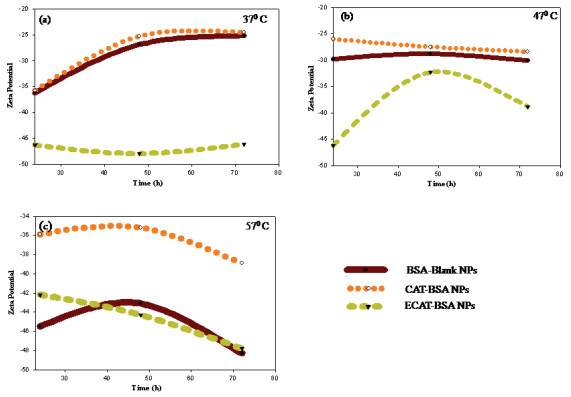

Figure 5: Zeta potential of blank-bovine serum albumin nanoparticles (BSA NPs), catechin-bovine serum albumin nanoparticles (CAT-BSA NPs) and epicatechin-bovine serum albumin nanoparticles (ECAT-BSA NPs) at different temperatures **(a)** 37 °C; **(b)** 47 °C; **(c)** 57 °C

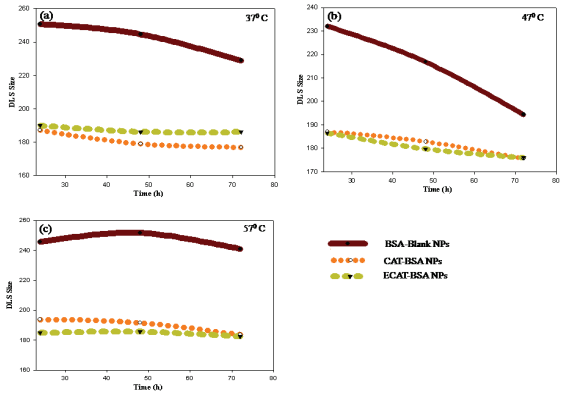

Figure 6: The DLS size of blank-bovine serum albumin nanoparticles (BSA NPs), catechin-bovine serum albumin nanoparticles (CAT-BSA NPs) and epicatechin-bovine serum albumin nanoparticles (ECAT-BSA NPs) at different temperatures **(a)** 37 °C; **(b)** 47 °C; **(c)** 57 °C

EXCLI Journal 2014;13:331-346 – ISSN 1611-2156
Received: January 31, 2014, accepted: February 27, 2014, published: April 01, 2014

the low EE of both the molecules CAT and ECAT in BSA NPs compared to various reported molecules could be attributed to their chemical nature. From nanobiotechnology perspective, the observed EE is still good for such easily oxidisable/degradable molecules.

In vitro release of CAT-BSA and ECAT-BSA NPs

The release of drugs depends upon the biodegradable nature of polymer, thermodynamic compatibility between polymers and drugs, nature of matrix, dilution of releasing medium and the interaction of encapsulated molecules with the nanomaterials (Park et al., 2005). Encapsulation of drugs on the NPs synthesized from such biodegradable polymers can easily control the rate of drug released, and the drug concentration (Kamaly et al., 2012). The release kinetics of drug changes when temperature and pH of releasing medium are altered and resulted pattern of release profile may be different from the physiological conditions (Bennet et al., 2012). The sustained release of drug from the NPs protects the drug from its fast metabolism and degradation (Kamaly et al., 2012).

In vitro release study of CAT-BSA, ECAT-BSA and BSA NPs was carried out in PBS and calculated using formula 3. The release kinetics of both the molecules was studied up to 48 hours (Figure 7, Figure S6). Initially for two hours the release of CAT was 10.5 %, while the release of ECAT was 29.2 % from the NPs in PBS. Rapid initial release is attributed to the fraction of the CAT and ECAT adsorbed or weakly bound to the large surface area of the NPs. Interestingly, the release of CAT from BSA NPs was increased to 35.6 % after 4 h whereas there was no change in release of ECAT upto 4 h of release.

The methods of drug incorporation in NPs have been reported to influence the release kinetics (Yoo et al., 1999). The drug adsorbed in the NPs has been reported to burst release up to 60-70 % followed by the remaining quite slow release. The chemically conjugated drugs in polymeric NPs have shown sustained release over many days (Fresta et al., 1995). The release profile of ECAT was slow between 8 to 12 h followed by fast release of molecules in release medium. Nature of polymer matrix also has influenced on the distribution of drug in NPs and their release (Niwa et al., 1993). The maximum release of CAT was 79 % after 42 h and that of ECAT was 75 % after18 h. Earlier studies also reported similar release of bioactive molecules from the BSA NPs (Fang et al., 2011; Abbasi et al., 2012). Folate-conjugated albumin NPs have been reported for slow release of etoricoxiband upto 72 h (Bilthariya et al., 2013). HSA NPs loaded with noscapine have been reported for 60 % release after 72 h (Sebak et al., 2010). BSA NPs were found to be capable of releasing CAT and ECAT in slow and sustained manner. The CAT and ECAT release from NPs follows prolonged and two phase release kinetics. Initial burst phase followed by slow and sustained phase. Initial burst phase is due to the CAT and ECAT physically adsorbed on the surface of BSA NPs. The CAT and ECAT bound in the core of BSA NPs were released in a slow and sustained manner. Aspirin loaded BSA NPs have also been re-

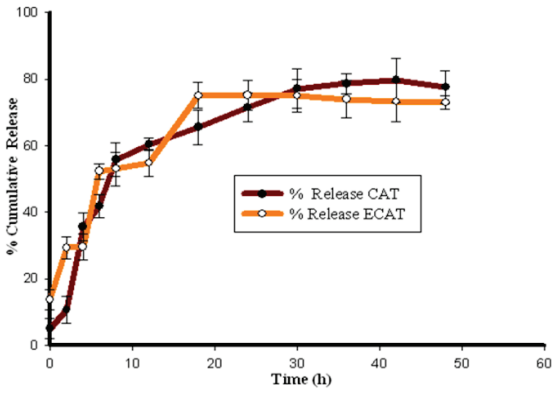

Figure 7: The release curve of catechin (CAT) and epicatechin (ECAT) using high performance liquid chromatography (HPLC) by plotting % cumulative release *vs* time. Values are the mean of three biological replicates ± standard error.

EXCLI Journal 2014;13:331-346 – ISSN 1611-2156
Received: January 31, 2014, accepted: February 27, 2014, published: April 01, 2014

ported for similar two phase release (Das et al., 2005).The release profile of both the molecules supported the use of synthesized nanomaterials for both *in vitro* and *in vivo* conditions.

Retention of antioxidant activity CAT, ECAT upon encapsulation on BSA NPs

DPPH (1,1-diphenyl-2-picrylhydrazyl) is a stable free radical containing spare electrons delocalization over the whole molecule. This electron delocalization gives a deep violet colour to it characterized by an absorption band at about 517 nm (Molyneux, 2004). The loss of this violet color is observed when a solution of DPPH is mixed with that of a molecule that can donate a hydrogen atom. The percentage of inhibition of DPPH was calculated by formula 4.

The CAT and ECAT are well known antioxidant molecules and used in food cocoa, vinegar and glycemic control (Zheng et al., 2013; Soobrattee et al., 2005; Amic et al., 2003). The solution of antioxidant molecules CAT and ECAT were incubated with DPPH, acting as a hydrogen atom donor, and thus a stable non-radical form of DPPH was obtained with simultaneous change from violet color to pale yellow and absorbance was decreased (Figure 8(a)). The CAT and ECAT contain labile hydrogen atoms and by liberation of these hydrogen atoms DPPH inhibition was obtained. This has also converted unstable CAT/ECAT into stable quinine moiety (Figure 8(b)). The lower inhibition of DPPH by the CAT BSA and ECAT BSA NPs compared to their unencapsulated analogue might be due to slow release of loaded molecules during the incubation period in dark or encapsulation might have hindered the availability of hydrogen radicals and provided protection to

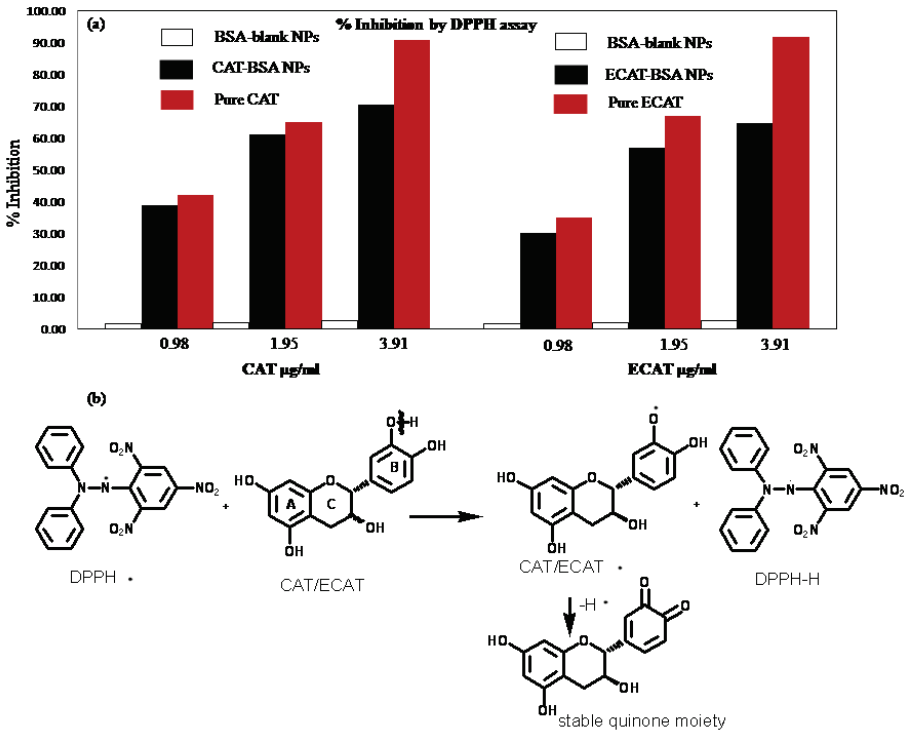

Figure 8: (a) Relative free radical scavenging potential of catechin (CAT), epicatechin (ECAT), catechin-bovine serum albumin (CAT-BSA) and epicatechin-bovine serum albumin (ECAT-BSA) by 2,2-Diphenyl-1-picrylhydrazyl (DPPH) assay. Upon encapsulation, the antioxidant activity of CAT and ECAT was slightly reduced in comparisons to pure CAT and ECAT. Active hydroxyl groups on CAT and ECAT quenched the free radical of DDPH turning its deep violet color to pale yellow. **(b)** the antioxidant mechanism of CAT/ECAT

CAT and ECAT from being oxidized. DPPH assay has been used earlier to evaluate the antioxidant activity of encapsulated molecules. The antioxidant activities of essential oil eugenol and carvacrol-grafted chitosan NPs have been reported using DPPH assay (Chen et al., 2009). Similarly, the antioxidant activity of quercitrin encapsulated in PLA NPs was assessed by DPPH assay (Kumari et al., 2011).

Efficacy of CAT and ECAT loaded BSA nanoparticles

Drug resistance is a major reason behind the treatment failure in several types of cancer including lung cancer (Sadhukha et al., 2013). Cell exhibits drug resistance which is governed by noncellular and cellular mechanisms (Andrew et al., 2006). Due to the multi-drug resistance the conventional drug delivery methods exhibit generally lower toxicity. The nanotechnology aspects like nanoencapsulation, liposomes, microspheres and targeted delivery could be useful to overcome the drug resistance and also enhance the efficacy of bioactive molecules (Davda and Labhasetwar, 2002). Therefore, this technology could be of great clinical significance because many bioactive molecules have low therapeutic indices.

Also the pay load of molecules in NPs should not be altered. It is necessity to maintain the functional values even after loading of molecules for such nano delivery systems (Brzoska et al., 2004; Yadav et al., 2013). The loaded CAT and ECAT maintained their functional activity after the encapsulation and *in vitro* release from BSA NPs. SRB assay was carried out to evaluate the efficacy of pure CAT, pure ECAT, CAT-BSA NPs, ECAT-BSA NPs and blank BSA NPs at various concentrations 50, 100, 150 and 200 µg/ml against A549 cells for 24, 48 and 72 h (Table 1). The percentage cellular inhibition was calculated by measuring the absorbance of respective incubated cells in the 96 well plates using formula 5. The CAT-BSA NPs showed maximum inhibition of A549 cells by 63.5 % at 50 µg/ml concentration while ECAT- BSA NPs showed maximum inhibition by 50.6 % at 200 µg/ml concentration after 72 h of incubation.

The pure CAT and ECAT have shown concentration dependent activity. Pure CAT and ECAT were observed to be inhibiting the growth of A549 cells to a lower extent in comparison to the CAT-BSA NPs and ECAT-BSA NPs. Among NPs, the efficacy of CAT-BSA NPs was found to be higher than ECAT-BSA NPs. The cellular efficacy study indicates that both the molecules have maintained their functional activity and showed greater inhibition of A549 cells after nanoencapsulated in BSA NPs.

CONCLUSIONS

In the current study, homogeneous CAT and ECAT encapsulated BSA NPs of less than 50 nm sizes were produced through desolvation method. The encapsulated CAT-BSA and ECAT-BSA NPs showed slow and sustained release of CAT and ECAT. Also, the BSA nanoencapsulation has been found to be improving the stability of these molecules at higher temperatures for longer duration. CAT-BSA and ECAT-BSA NPs show improved scavenging activity and efficacy of loaded molecule against A549 cells. This study has thus documented the potential use of CAT and ECAT in food and nutraceuticals as well as medical field.

ACKNOWLEDGEMENTS

Authors are thankful to the Director, CSIR-IHBT, palampur for continuous support and encouragment. RY acknowledges Council of Scientific and Industrial Research, India for providing Senior Research Fellowship. The financial support from Council of Scientific and Industrial Research, India in the form of BSC-112 is duly acknowledged. The CSIR-IHBT communication number of this article is 3631.

EXCLI Journal 2014;13:331-346 – ISSN 1611-2156
Received: January 31, 2014, accepted: February 27, 2014, published: April 01, 2014

Table 1: Comparative *in vitro* efficacy of pure CAT, pure ECAT, CAT-BSA NPs, ECAT-BSA NPs and blank BSA NPs against A549 cells. Values are the mean of three biological replicates ± standard error.

Sample	Concentration (µg/ml)	A549 (% Growth Inhibition with SD[#])		
		24 h	48 h	72 h
Pure CAT	50	19.7 ± 3.5	8.6 ± 2.1	11.6 ± 4.0
	100	28.5 ± 1.0	11.2 ± 4.1	18.4 ± 2.4
	150	22.0 ± 2.9	16.2 ± 2.4	12.9 ± 3.1
	200	29.1 ± 4.8	20.8 ± 3.8	27.5 ± 2.5
Pure ECAT	50	24.4 ± 1.9	10.5 ± 0.3	9.3 ± 4.3
	100	25.0 ± 4.1	7.0 ± 2.9	17.8 ± 3.4
	150	14.5 ± 1.9	10.6 ± 2.4	9.2 ± 5.0
	200	21.0 ± 3.1	17.7 ± 2.7	31.5 ± 2.9
CAT NPs	50	6.4 ± 0.4	35.1 ± 1.1	63.5 ± 1.1
	100	14.5 ± 3.1	32.2 ± 3.1	31.7 ± 2.8
	150	12.5 ± 2.9	7.9 ± 3.1	21.5 ± 0.8
	200	22.2 ± 3.7	15.6 ± 1.2	56.4 ± 2.9
ECAT NPs	50	7.9 ± 4.3	35.1 ± 2.1	3.9 ± 1.8
	100	4.5 ± 3.6	32.2 ± 0.4	6.7 ± 4.4
	150	3.1 ± 3.4	7.9 ± 2.4	15.6 ± 2.0
	200	16.4 ± 1.9	15.6 ± 0.8	50.6 ± 1.6
Blank BSA NPs	50	2.7 ± 1.3	17.9 ± 0.4	14.6 ± 3.4
	100	2.8 ± 3.3	0.4 ± 2.3	2.0 ± 1.6
	150	0.0 ± 4.2	0.0 ± 1.7	0.0 ± 2.9
	200	8.4 ± 3.4	27.4 ± 4.2	42.0 ± 2.6
Vinblastin	(1µM)	65.7 ± 2.3	74.9 ± 1.8	84.8 ± 1.4

SUPPLEMENTARY INFORMATION

Additional supplementary information may be found in the online version of this article.

REFERENCES

Abbasi S, Paul A, Shao W, Prakash S. Cationic albumin nanoparticles for enhanced drug delivery to treat breast cancer: preparation and in vitro assessment. J Drug Del 2012;2012:1-8.

Albanese A, Tang PS, Chan WCW. The effect of nanoparticle size, shape, and surface chemistry on biological systems. Annu Rev Biomed Eng 2012;14: 1-16.

Amic D, Davidovic D, Bešlo D, Trinajstic N. Structure-radical scavenging activity relationships of flavonoids. Croat Chem Acta 2003;76:55-61.

Andrew HW, Rauth M, Bendayan R, Manias JL, Ramaswamy M, Liu Z et al. A new polymer-lipid hybrid nanoparticle system increases cytotoxicity of doxorubicin against multidrug-resistant human breast cancer cells. Pharm Res 2006;23:1574-84.

Avgoustakis K, Beletsi A, Panagi Z, Klepetsanis P, Karydas AG, Ithakissios DS. PLGA-mPEG nanoparticles of cisplatin: in vitro nanoparticle degradation, in vitro drug release and in vivo drug residence in blood properties. J Control Release 2002;79:123-35.

Bansal A, Kapoor DN, Kapil R, Chhabra N, Dhawan S. Design and development of paclitaxel-loaded bovine serum albumin nanoparticles for brain targeting. Acta Pharm 2011;61:141-56.

Bark KM, Yeom JE, Yang JI, Yang IJ, Park CH, Park HR. Spectroscopic studies on the oxidation of catechin in aqueous solution. Bull Korean Chem Soc 2011;32:3443-47.

Bennet D, Marimuthu M, Kim S, An J. Dual drug-loaded nanoparticles on self-integrated scaffold for controlled delivery. Int J Nanomed 2012;7:3399-19.

Bilthariya U, Jain N, Rajoriya V, Jain AK. Folate-conjugated albumin nanoparticles for rheumatoid arthritis-targeted delivery of etoricoxib. Drug Dev Ind Pharm (2013) (Epub ahead of print) (doi: 10.3109/03639045.2013.850705).

Brzoska M, Langer K, Coester C, Loitsch S, Wagner TOF, Mallinckrodta CV. Incorporation of biodegradable nanoparticles into human airway epithelium cells-in vitro study of the suitability as a vehicle for drug or gene delivery in pulmonary diseases. Biochem Biophys Res Commun 2004;318:562-70.

Catterall F, King LJ, Clifford MN, Ioannides C. Bioavailability of dietary doses of 3H-labelled tea antioxidants (+)-catechin and (-)-epicatechin in rat. Xenobiotica 2003;33:743-53.

Chen F, Shi Z, Neoh KG, Kang ET. Antioxidant and antibacterial activities of eugenol and carvacrol-grafted chitosan nanoparticles. Biotechnol Bioeng 2009;104:30-39.

Chen YC, Yu SH, Tsai GJ, Tang DW, Mi FL, Peng YP. Novel technology for the preparation of self-assembled catechin/gelatin nanoparticles and their characterization. J Agri Food Chem 2010;58:6728-34.

Chitkara D, Kumar N. BSA-PLGA-based core-shell nanoparticles as carrier system for water-soluble drugs. Pharm Res 2013;30:2396-409.

Chu KO, Wang CC, Rogers MS, Choy KW, Pang CP. Determination of catechins and catechin gallates in biological fluids by HPLC with coulometric array detection and solid phase extraction. Anal Chim Acta 2004;510:69-76.

Das S, Banerjee R, Bellare J. Aspirin loaded albumin nanoparticles by coacervation: implications in drug delivery. Trend Biomater Artif Org 2005;18:203-12.

Davda J, Labhasetwar V. Characterization of nanoparticle uptake by endothelial cells. Int J Pharm 2002;233:51-9.

Derakhshandeh K, Erfan M, Dadashzadeh S. Encapsulation of 9-nitrocamptothecin, a novel anticancer drug, in biodegradable nanoparticles: factorial design, characterization and release kinetics. Eur J Pharm Biopharm 2007;66:34-41.

Dube A, Ng K, Nicalazgo JA, Larson I. Effective use of reducing agents and nanoparticle encapsulation in stabilising catechins in alkaline solution. Food Chem 2010;122:662-7.

Dufort S, Sancey L, Coll JL. Physico-chemical parameters that govern nanoparticles fate also dictate rules for their molecular evolution. Adv Drug Deliv Rev 2012;64:179-89.

Elzoghby AO, Samy WM, Elgindy NA. Albumin-based nanoparticles as potential controlled release drug delivery systems. J Control Release 2012;157:168-82.

Fang R, Jing H, Chai Z, Zhao G, Stoll S, Ren F et al. Design and characterization of protein-quercetin bioactive nanoparticles. J Nanobiotechnol 2011;9:1-19.

Freitas C, Müller RH. Effect of light and temperature on zeta potential and physical stability in solid lipid nanoparticle (SLN™) dispersions. Int J Pharm 1998;168:221-9.

Fresta M, Puglisi G, Giammona G, Cavallaro G, Micali N, Furneri PM. Pefloxacin mesilate- and ofloxacin-loaded polyethylcyanoacrylate nanoparticles; characterization of the colloidal drug carrier formulation. J Pharm Sci 1995;84:895-901.

Haris PI. Can infrared spectroscopy provide information on protein-protein interactions? Biochem Soc Trans 2010;38:940-6.

Huang X, Teng X, Chen D, Tang F, He J. The effect of the shape of mesoporous silica nanoparticles on cellular uptake and cell function. Biomaterials 2010;31:438-48.

Inniguez-Franco F, Soto-Valdez H, Peralta E, Ayala-Zavala JF, Auras R, Gámez-Meza N. Antioxidant activity and diffusion of catechin and epicatechin from antioxidant active films made of poly(L-lactic acid). J Agric Food Chem 2012;60:6515-23.

Jun JY, Nguyen HH, Paik SYR, Chun HS, Kang BC, Ko S. Preparation of size-controlled bovine serum albumin (BSA) nanoparticles by a modified desolvation method. Food Chem 2011;127:1892-8.

Kamaly N, Xiao Z, Valencia PM, Radovic-Moreno AF, Farokhzad OC. Targeted polymeric therapeutic nanoparticles: design, development and clinical translation. Chem Soc Rev 2012;41:2971-3010.

Knekt P, Jarvinen R, Reunanen A, Maatela J. Flavonoid intake and coronary mortality in Finland: a cohort study. Br Med J 1996;312:478-81.

Koo MW, Cho CH. Pharmacological effects of green tea on the gastrointestinal system. Eur J Pharmacol 2004;500:177-85.

Kumari A, Yadav SK, Yadav SC. Biodegradable polymeric nanoparticles based drug delivery systems. Coll Surf B Biointerfaces 2010a;75:1-18.

Kumari A, Yadav SK, Pakade YB, Singh B, Yadav SC. Development of biodegradable nanoparticles for delivery of quercetin. Colloid Surf B Biointerfaces 2010b;80:184-92.

Kumari A, Yadav SK, Pakade YB, Kumar V, Singh B, Chaudhary et al. Nanoencapsulation and characterization of *Albizia chinensis* isolated antioxidant quercitrin on PLA nanoparticles. Colloid Surf B Biointerfaces 2011;82:224-32.

Kumari A, Kumar V, Yadav SK. Plant extract synthesized PLA nanoparticles for controlled and sustained release of quercetin: a green approach. PLoS one 2012;7:e41230.

Kvıtek L, Panacek A, Soukupova J, Kolar M, Vecerova R, Prucek R et al. Effect of surfactants and polymers on stability and antibacterial activity of silver nanoparticles (NPs). J Phys Chem C 2008;112:5825-34.

Li DL, Li XM, Peng ZY, Wang BG. Flavanol derivatives from *Rhizophora stylosa* and their DPPH radical scavenging activity. Molecules 2007;12: 1163-9.

Li D, Martini N, Wu Z, Wen J. Development of an isocratic HPLC method for catechin quantification and its application to formulation studies. Fitoterapia 2012;83:1267-74.

Li FQ, Su H, Wang J, Liu JY, Zhu QG, Fei YB et al. Preparation and characterization of sodium ferulate entrapped bovine serum albumin nanoparticles for liver targeting. Int J Pharm 2008;349:274-82.

Ma R, Levard C, Marinakos SM, Cheng Y, Liu J, Michel FM et al. Size-controlled dissolution of organic-coated silver nanoparticles. Environ Sci Technol 2012;46:752-9.

Madlova M, Jones SA, Zwerschke I, Ma Y, Hider RC, Forbes B. Poly (vinyl alcohol) nanoparticle stability in biological media and uptake in respiratory epithelial cell layers *in vitro*. Eur J Pharm Biopharm 2009;72:437-43.

Maghsoudi A, Shojaosadati SA, Farahani EV. 5-Fluorouracil-loaded BSA nanoparticles: formulation optimization and in vitro release study. AAPS Pharm Sci Tech 2008;9:1092-6.

Maoela MS, Arotiba OA, Baker PGL, Mabusela WT, Jahed N, Songa EA et al. Electroanalytical determination of catechin flavonoid in ethyl acetate extracts of medicinal plants. Int J Electrochem Sci 2009;4:1497-510.

Maurya PK, Rizvi SI. Protective role of tea catechins on erythrocytes subjected to oxidative stress during human aging. Nat Prod Res 2009;23:1072-9.

McGugan EA. Hyperpyrexia in the emergency department. Emerg Med (Fremantle) 2001;13:116-20.

Moghimi SM, Hunter AC, Murray JC. Long-circulating and target-specific nanoparticles: theory to practice. Pharmacol Rev 2001;53:283-318.

Molyneux P. The use of the stable free radical diphenylpicrylhydrazyl (DPPH) for estimating antioxidant activity. Songklanakarin J Sci Technol 2004; 26:211-9.

Muller BG, Leuenberger H, Kissel T. Albumin nanospheres as carriers for passive drug targeting: an optimized manufacturing technique. Pharm Res 1996;13:1332-7.

Munin A, Edwards-Levy F. Encapsulation of natural polyphenolic compounds; a review. Pharmaceutics 2011;3:793-829.

Muthu MS, Feng SS. Pharmaceutical stability aspects of nanomedicines. Nanomedicine 2009;4:857-60.

Nagarajan S, Nagarajan R, Braunhut SJ, Bruno F, McIntosh D, Samuelson L et al. Biocatalytically oligomerized epicatechin with potent and specific antiproliferative activity for human breast cancer cells. Molecules 2008;13:2704-16.

Nel AE, Madler L, Velegol D, Xia T, Hoek EMV, Somasundaran P et al. Understanding biophysicochemical interactions at the nano-bio interface. Nat Mater 2009;8:543-57.

Niwa T, Takeuchi H, Hino T, Kunou N, Kawashima Y. Reparations of biodegradable nanospheres of water-soluble and insoluble drugs with D,L-lactide/ glycolide copolymer by a novel spontaneous emulsification solvent diffusion method and the drug release behavior. J Control Release 1993;25:89-98.

Park JH, Ye M, Park K. Biodegradable polymers for microencapsulation of drugs. Molecules 2005;10: 146-61.

Patil GV. Biopolymer albumin for diagnosis and in drug delivery. Drug Dev Res 2003;58:219-47.

Pool H, Quintanar D, Figueroa JD, Mano CM, Bechara JEH, Godınez LA et al. Antioxidant effects of quercetin and catechin encapsulated into PLGA nanoparticles. J Nanomater 2012;2012:1-12 (article No. 86).

Reis CP, Neufeld RJ, Ribeiro AJ, Veiga F. Nanoencapsulation I. Methods for preparation of drug-loaded polymeric nanoparticles. Nanomed Nanotechnol Biol Med 2006;2:8-21.

Sadhukha T, Wiedmann TS, Panyam J. Inhalable magnetic nanoparticles for targeted hyperthermia in lung cancer therapy. Biomaterials 2013;34:5163-71.

Sailja AK, Amareshwar P. Prepration of BSA nanoparticles by desolvation technique using acetone as desolvating agent. Int J Pharm Sci Nanotech 2012; 5:1643-7.

Sebak S, Mirzaei M, Malhotra M, Kulamarva A, Prakash S. Human serum albumin nanoparticles as an efficient noscapine drug delivery system for potential use in breast cancer: preparation and *in vitro* analysis. Int J Nanomed 2010;5:525-32.

Shafique K, McLoone P, Qureshic K, Leungd H, Hart C, Morrison DS. Tea consumption and the risk of overall and grade specific prostate cancer: a large prospective cohort study of Scottish men. Nutr Cancer 2012;64:790-7.

Shang L, Wang Y, Jiang J, Dong S. pH-dependent protein conformational changes in albumin:dold nanoparticle bioconjugates: A spectroscopic study. Langmuir 2007;23:2714-21.

Singh AV, Bandgar BM, Kasture M, Prasad BLV, Sastry M. Synthesis of gold, silver and their alloy nanoparticles using bovine serum albumin as foaming and stabilizing agent. J Mater Chem 2005;15: 5115-21.

Soobrattee MA, Neergheen VS, Luximon-Ramma A, Aruoma OI, Bahorun T. Phenolics as potential antioxidant therapeutic agents: mechanism and actions. Mut Res 2005;579:200-13.

Volf I, Ignat I, Neamtu M, Popa VI. Thermal stability, antioxidant activity, and photo-oxidation of natural polyphenols. Chem Pap 2014;68:121-9.

Von Burkersroda F, Schedl L, Göpferich A. Why degradable polymers undergo surface erosion or bulk erosion. Biomaterials 2002;23:4221-31.

Xie L, Tong W, Yu D, Xu J, Li J, Gao C. Bovine serum albumin nanoparticles modified with multilayers and aptamers for pH-responsive and targeted anti-cancer drug delivery. J Mater Chem 2012;22: 6053-60.

Yadav SC, Kumari A, Yadav R. Development of peptide and protein nanotherapeutics by nanoencapsulation and nanobioconjugation. Peptides 2011;32: 173-87.

Yadav R, Kumar D, Kumari A, Yadav SK. Encapsulation of podophyllotoxin and etoposide in biodegradable poly-D,L-lactide nanoparticles improved their anticancer activity. J Microencapsul (2013) (Epub ahead of print) (doi: 10.3109/02652048.2013. 834988).

Yogasundaram H, Bahniuk MS, Singh HD, Aliabadi HM, Uludağ H, Unsworth LD. BSA nanoparticles for siRNA delivery: coating effects on nanoparticle properties, plasma protein adsorption, and *in vitro* siRNA delivery. Int J Biomater 2012;2012:1-10.

Yoo HS, Oh JE, Lee KH, Park TG. Biodegradable nanoparticles containing doxorubicin-PLGA conjugate for sustained release. Pharm Res 1999;16:1114-8.

Zambaux MF, Bonneaux F, Gref R, Dellacherie E, Vigneron C. Preparation and characterization of protein C-loaded PLA nanoparticles. J Control Release 1999;60:179-88.

Zhao D, Zhao X, Zu Y, Li J, Zhang Y, Jiang R et al. Preparation, characterization, and in vitro targeted delivery of folate-decorated paclitaxel-loaded bovine serum albumin nanoparticles. Int J Nanomed 2010; 5:669-77.

Zheng XX, Xu YL, Li SH, Hui R, Wu YJ, Huang XH. Effects of green tea catechins with or without caffeine on glycemic control in adults: a meta-analysis of randomized controlled trials. Am J Clin Nutr 2013;97:750-62.